

PhysFormer: A Physics-Embedded Generative Model for Physically Self-Consistent Spectral Synthesis

Siqi Wang¹, Mengmeng Zhang¹, Yude Bu^{1,*}, Chaozhou Mou²

¹School of Mathematics and Statistics, Shandong University, Weihai, 264209, Shandong, China

²Weihai Institute for Interdisciplinary Research, Shandong University, Weihai 264209, Shandong, China

{202417877, mmzhang}@mail.sdu.edu.cn,

{buyude, mouchaozhou}@sdu.edu.cn (*Corresponding author: Yude Bu)

Abstract

In scientific and engineering domains, modeling high-dimensional complex systems governed by partial differential equations (PDEs) remains challenging in terms of physical consistency and numerical stability. However, existing approaches, such as physics-informed neural networks (PINNs), typically rely on known physical fields or coefficients and enforce physical constraints via external loss functions, which can lead to training instability and make it difficult to handle high-dimensional or unobservable scenarios. To this end, we propose PhysFormer, a generative modeling framework that is self-consistent at both the data and physical levels. PhysFormer leverages a low-dimensional, physically interpretable latent space to learn key physical quantities directly from data without requiring known high-dimensional physical field parameters, and embeds the physical process of radiative flux generation within the network to ensure the physical consistency of the generated spectra. In high-dimensional, degenerate inversion tasks, PhysFormer constrains generation within physical limits and enhances spectral fidelity and inversion stability under varying signal-to-noise ratios (SNRs). More broadly, this approach shifts the physical processes from external loss functions into the generative mechanism itself, providing a physically consistent generative modeling paradigm for complex systems involving unknown or unobservable physical quantities.

1 Introduction

Accurately modeling and simulating complex systems is crucial in various scientific and engineering fields [Wan *et al.*, 2025]. These systems are typically governed by partial differential equations (PDEs) and intricate physical processes, making it persistently challenging to achieve stable and scalable modeling while maintaining physical consistency. In recent years, physics-informed neural networks (PINNs) have sought to incorporate physical laws into deep learning models. Owing to their scalability [Meng *et al.*, 2020] and flexibility [Zhu *et al.*, 2022], they have demonstrated promise in

solving differential equations and inverse problems [Raissi *et al.*, 2020]. However, most existing PINN-based methods mainly rely on external loss functions for physical constraints, making it difficult to automatically discover and embed physically consistent network structures [Liu *et al.*, 2025]. Meanwhile, constructing physical loss functions typically requires known and explicitly parameterizable physical quantities, such as known equation coefficients, initial conditions or boundary conditions [Raissi *et al.*, 2019; Cheridito *et al.*, 2025], which are not always available in real-world applications. As a result, the applicability of PINNs in more complex scenarios is limited.

Particularly in astrophysics, climate science, and plasma physics, many physical quantities required for solving governing equations—such as opacity, absorption coefficients—are often not directly observable. In such problems, conventional PINNs primarily act as equation solvers augmented with physical constraints. They struggle to function as data-driven models capable of discovering underlying physical structures. When such models are extended to ultra-high-dimensional output tasks, such as high-resolution spectral modeling, their limitations become increasingly pronounced. These issues manifest as unstable training and degraded generalization performance. In inverse problems, the models also tend to converge to local optima that satisfy PDE residuals but lack physical meaning [Nasir *et al.*, 2025].

Stellar spectral modeling provides a prototypical and highly challenging research scenario for studying such problems. The structure of stellar atmospheres is inherently constrained by established physical laws, such as the radiative transfer equation and the energy theorem. Mapping a small set of stellar parameters accurately to ultra-high-dimensional stellar spectra not only requires the model to have strong deep learning fitting capabilities but also to preserve the intrinsic physical consistency of the stellar atmosphere. Moreover, PINNs require the physical structure to be predefined. Therefore, they are not well suited for scenarios like stellar spectral modeling, where data are scarce and physical quantities must be inferred directly from the data.

To overcome these limitations, we propose a generative modeling framework that is self-consistent at both the data and physical levels. It extends the application of PINNs from equation solvers constrained by physics to physically consistent generative models. Rather than treating established

physical laws as external constraints, physical processes are embedded directly into the network as part of its generative mechanism. This design does not rely on predefined PDE coefficients or scarce physical parameters. It can generate high-precision spectra that are consistent both numerically and with physical constraints.

We validate the effectiveness of the proposed framework on the PHOENIX theoretical spectral dataset spanning the ultraviolet to infrared bands, and the experimental results demonstrate that the method achieves superior stability, accuracy, and robustness in both high-dimensional spectral generation and parameter inversion tasks. In summary, we make the following contributions:

- We propose a physically self-consistent framework at both data and physical levels, which is capable of learning representations of key physical quantities directly from data. It reduces the dependence of PINNs on fixed PDE coefficients and predefined physical parameters.
- PhysFormer embeds key physical processes, such as the radiative transfer equation and the energy theorem, directly into the network architecture. Instead of merely adding physical laws to the network loss function as external constraints, it enables physically consistent forward spectral generation.
- PhysFormer achieves high-precision, efficient modeling and parameter inference for ultra-high-dimensional stellar spectra. It provides a flexible spectral framework that is self-consistent at both the data and physical levels for stellar spectral modeling tasks.

2 Related Work

PINNs provide a general framework that integrates physical laws into the neural network training process as loss functions to solve PDE-driven forward and inverse problems [Jagtap and Karniadakis, 2020; Jagtap *et al.*, 2020; Mao *et al.*, 2020]. Existing methods can be broadly divided into two categories. The first category focuses on forward problems, aiming to approximate PDE solutions under fixed physical conditions with the associated physical fields and coefficients typically assumed to be known [Raissi *et al.*, 2019]. The second category extends PINNs to inverse problems, in which some unknown parameters are treated as learnable variables and optimized jointly with the network weights to achieve parameter identification and system inversion [Yang *et al.*, 2021]. Although PINNs have partially overcome the curse of dimensionality and are capable of approximating PDE solutions [De Ryck and Mishra, 2022], most existing methods still rely on specifying the physical structure prior to training, which may limit their applicability in high-dimensional or partially unobservable physical fields.

To improve the data efficiency and physical consistency of PINNs, one class of methods attempts to automatically discover network structures through teacher-student network distillation [Liu *et al.*, 2025], and then extract physically meaningful structures through clustering and parameter reconstruction. However, such methods typically require substantial prior knowledge of governing equations, which limits their scalability in high-dimensional or very long sequence

tasks. In addition, physics-encoded approaches directly embed physical constraints into the network architecture, such as PDE operators, conservation laws, and boundary conditions [Long *et al.*, 2019; Rao *et al.*, 2023; Mi and Sun, 2024; Zeng *et al.*, 2025].

Stellar spectral modeling represents a highly challenging application scenario for physics-informed learning methods. Traditional template-matching methods are computationally expensive and difficult to scale. In recent years, deep learning approaches have achieved notable progress in this field. For example, [Sedaghat *et al.*, 2021] trained an encoder-decoder architecture on a large stellar spectral dataset for self-supervised spectral reconstruction. [Li *et al.*, 2022] developed a deep convolutional neural network to predict key stellar atmospheric parameters. [Corral *et al.*, 2023] trained deep learning models on a database of synthetic spectra. However, these approaches are primarily data-driven, and the learned features lack explicit physical interpretability.

For forward generation and parameter inversion tasks, [Ting *et al.*, 2019] proposed a framework that performs forward modeling from parameters to theoretical spectral fluxes and then conducts parameter inversion on observed spectra, but the model itself remains purely data-driven. In recent years, PINNs have also been partially applied to stellar spectral modeling. [Dahlbüdding *et al.*, 2024] employed PINNs for radiative transfer modeling of exoplanetary atmospheres. [Li *et al.*, 2025] incorporated the hydrostatic equilibrium equation into the network architecture to generate stellar atmospheric structures. However, these methods rely on physical quantities provided by theoretical models and have not yet addressed the modeling challenges arising from unknown or unobservable physical quantities.

3 Methodology

3.1 Problem Formulation

This paper focuses on a physics-constrained generative modeling and parameter inversion problem, with its application background rooted in stellar spectral modeling. The goal is, given a set of fundamental stellar atmospheric parameters

$$\theta = (T_{\text{eff}}, \log g, [\text{Fe}/\text{H}], [\alpha/\text{Fe}]) \in \mathbb{R}^4, \quad (1)$$

to generate the corresponding high-resolution stellar spectrum $\mathbf{F} \in \mathbb{R}^W$, covering an ultra-wide wavelength range across ultraviolet, optical, and infrared bands. The core challenge lies in the fact that stellar atmospheric structures are inherently constrained by the radiative transfer equation and the energy theorem, while key physical quantities—such as true absorption coefficients, scattering coefficients, and radiative intensity—are difficult to obtain directly. Consequently, the applicability of PINNs to high-dimensional spectral modeling and inversion tasks remains limited.

To this end, we propose a physically self-consistent generative modeling framework that learns physically meaningful latent representations directly from data, without assuming prior knowledge of physical field parameters, while explicitly embedding the physical generation process into the network architecture.

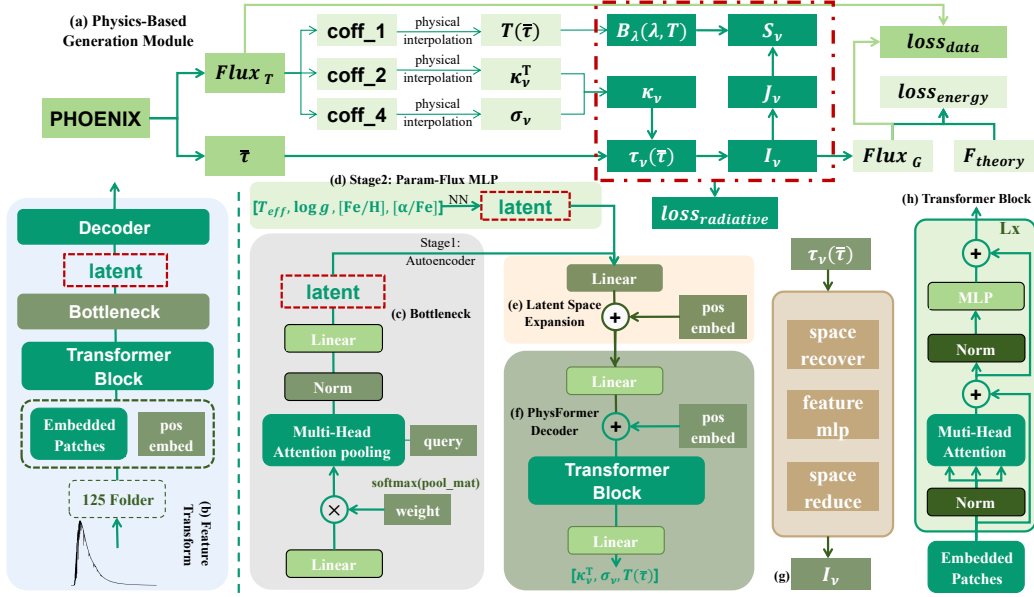


Figure 1: The architecture of PhysFormer. (a) Physical generation module that embeds physical processes directly into the network architecture. (b) Physically consistent spectral autoencoder. (c) Bottleneck architecture for generating a low-dimensional physical latent space. (d) Mapping network from stellar fundamental parameters to the physical latent space. (e) Latent Space Expansion Module. (f) PhysFormer decoder, used to generate key physical quantities required for subsequent physical computations. (g) Radiative Intensity Generation Module. (h) Transformer Block structure.

3.2 PhysFormer Architecture

PhysFormer (Figure 1) adopts a three-stage strategy: (1) physics-aware autoencoder pretraining, in which a bottleneck structure is introduced to learn a low-dimensional latent representation with physical interpretability; (2) parameter-to-latent mapping, where the spectral input is replaced by four-dimensional stellar parameters while the autoencoder is frozen; (3) parameter inversion, in which the trained PhysFormer is fixed and stellar parameters are optimized via χ^2 minimization. Overall, the model can be regarded as a physics-embedded conditional generative model that learns latent physical fields. An embedded physical generator takes the latent representation as input and data-drivenly produces the intermediate physical quantities required by the radiative transfer equation and the energy theorem, followed by numerical integration to obtain the final spectrum. In this framework, physical laws are incorporated as integral components of the generative process rather than imposed as external loss terms, thereby promoting consistency between data fidelity and physical validity in the generated spectra.

3.3 Physically consistent spectral autoencoder

Physics-Bottleneck Encoding Block

In the encoder, this work adopts an architecture similar to Vision Transformer [Dosovitskiy *et al.*, 2021], where the input spectrum is first partitioned into N non-overlapping patches along the spectral dimension. Multiple Transformer blocks are then applied for feature transformation to capture long-range dependencies across wavelengths. To mitigate the learning difficulties associated with directly mapping low-dimensional parameters to high-dimensional spec-

tra, we introduce a token-level latent bottleneck to compress high-dimensional token sequences into a low-dimensional latent space with physically meaningful structure [Jaegle *et al.*, 2021]:

$$\mathbf{Z}_{tok} = \mathcal{B}(\mathbf{Z}_e), \quad \mathbf{Z}_{tok} \in \mathbb{R}^{B \times K \times d_b}, \quad K \ll N. \quad (2)$$

Here, $\mathcal{B}(\cdot)$ denotes the bottleneck mapping operator, and d_b represents the dimensionality of the latent-token mapping. Building on this, we draw on the core idea of β -VAE [Higgins *et al.*, 2017] to further compress the K latent tokens into a one-dimensional global latent variable $Z_b \in \mathbb{R}^{B \times 1}$. This structure forces the model to encode full-spectrum information within a limited latent space, thereby facilitating the learning of stable and transferable physical representations that lay the foundation for subsequent parameter-driven generation.

Physics-Decoded Block

In the decoding stage, the low-dimensional latent representation is first dimensionally aligned with the number of patches in the original spectrum:

$$\tilde{\mathbf{Z}}_{tok} = \mathcal{U}(\mathbf{Z}_b) \in \mathbb{R}^{B \times N \times d_b}, \quad (3)$$

where $\mathcal{U}(\cdot)$ denotes a token expansion operator implemented via a linear mapping. Subsequently, the expanded latent variables are projected into the decoder embedding space and augmented with positional encodings (Z_d). They are then processed by Transformer blocks and linearly mapped to generate high-resolution, wavelength-wise distributions of physical parameters required by the subsequent physics module, including true absorption coefficients, scattering coefficients, and temperature distributions:

$$\{\kappa, \sigma, \mathbf{T}\} = \mathcal{H}(Z_d), \quad (4)$$

where $\mathcal{H}(\cdot)$ denotes the physical decoding head. This process is consistent with the paradigm in neural operator methods, which generate high-dimensional physical fields from low-dimensional variables [Li *et al.*, 2021].

Generative Physical Module

Physically Consistent Generative Spectral Modeling. After obtaining data-driven intermediate physical quantities, PhysFormer generates spectra using differentiable physics-inspired operators. First, a physically motivated optical depth interpolation expands the low-dimensional parameters to the full optical depth, capturing their variation with depth. It then computes frequency-dependent optical depth, radiation intensity, and their angular averages, and finally generates the emergent spectral flux via numerical integration under the plane-parallel atmosphere assumption.

The propagation path of the optical depth is discretized into L optical layers $\{s_i\}_{i=1}^L$, and the optical depth at a given frequency can be approximated in the form of a cumulative sum:

$$\tau_{\nu,i} = \sum_{k=1}^i \chi_{\nu,k} \Delta s_k, \quad \Delta s_k = s_k - s_{k-1}. \quad (5)$$

Here, $\chi_{\nu} = \kappa_{\nu} + \sigma_{\nu}$, which is constrained to be non-negative.

The radiation intensity I_{ν} depends on both the optical depth τ and the directional cosine $\mu = \cos \theta$. We parameterize I_{ν} using a lightweight convolutional neural network, such that

$$I_{\nu}(\tau_{\nu}, \mu) \approx \mathcal{N}_I \left(\frac{\tau_{\nu}}{\mu} \right). \quad (6)$$

Here, $\frac{\tau_{\nu}}{\mu}$ represents the effective optical depth when radiation propagates along different directions. This modeling approach preserves the physical dependency of radiation intensity on both optical depth and direction.

We discretize the angular integration using Gauss–Legendre quadrature [Press and Teukolsky, 2007]. $\{\mu_i, w_i\}_{i=1}^{N_{\mu}}$ denote the discrete angular points and their corresponding quadrature weights, respectively. The generated flux F_{ν} can be approximated as:

$$F_{\nu} = 2\pi \int_{-1}^1 I_{\nu} \mu d\mu. \quad (7)$$

Radiative Transfer Equation. The study of radiative transfer is crucial in many scientific fields, including astrophysics [Mishra and Molinaro, 2021]. In this work, we introduce a differentiable RTE residual as a physics-based regularization term, encouraging the evolution of radiation intensity with optical depth to remain consistent with physical laws:

$$\mathcal{R}_{\text{RTE}} = \frac{dI_{\nu}}{d(\tau_{\nu}/\mu)} e^{-\frac{\tau_{\nu}}{\mu}} - I_{\nu} e^{-\frac{\tau_{\nu}}{\mu}} + S_{\nu} e^{-\frac{\tau_{\nu}}{\mu}}. \quad (8)$$

Here, S_{ν} denotes the source function. The formulation penalizes physically inconsistent radiation transport by minimizing the RTE residual during training.

Energy Theorem. In stellar atmosphere modeling, it is necessary that the generated spectrum remains compatible

with the total radiative energy within a given wavelength range based on the energy balance relation. We introduce an energy theorem residual based on the Stefan–Boltzmann law and Planck’s formula [Hubeny and Mihalas, 2014]:

$$\mathcal{R}_{\text{ET}} = \int_{\nu_1}^{\nu_2} F_{\nu}(\nu, T) d\nu - \sigma T^4. \quad (9)$$

Here, ν_1 and ν_2 represent the specific wavelength range.

These physics-based losses serve only as auxiliary regularization during training. The physical processes themselves are explicitly embedded in the forward generative pipeline rather than being imposed solely through loss functions.

Mapping from Parameters to the Physical Latent Space

In the forward modeling stage, PhysFormer generates high-dimensional stellar spectra from low-dimensional stellar parameters. The stellar parameter vector is defined as

$$\mathbf{p} = (T_{\text{eff}}, \log g, [\text{Fe}/\text{H}], [\alpha/\text{Fe}]). \quad (10)$$

Given that the physics-aware autoencoder has learned a low-dimensional latent space encoding physical information, its parameters are frozen during this stage to maintain a consistent latent structure. A lightweight MLP is used to map parameters into this latent space, enabling parameter-conditioned spectral generation. This design alleviates the complexity of directly mapping low-dimensional parameters to high-dimensional spectra while preserving the physical structure and stability of the latent space.

Physics-consistent stellar parameter inversion

In the parameter inversion task, PhysFormer is regarded as an end-to-end differentiable physical forward model. To simulate observational conditions, Gaussian noise is added to the theoretical spectra, and stellar parameters p are estimated by minimizing the χ^2 objective:

$$\mathcal{L}_{\chi^2}(p) = \sum_{\nu=1}^W \frac{(F_{\nu}^{\text{obs}} - \hat{F}_{\nu}(p))^2}{\sigma_{\nu}^2}. \quad (11)$$

Here, F_{ν}^{obs} represents the simulated observed spectrum, $\hat{F}_{\nu}(p)$ denotes the physically consistent generated spectrum, and σ_{ν}^2 is the variance of the added noise, determined by the specified signal-to-noise ratio (SNR).

During the inversion, the forward model parameters are fixed, and only the stellar parameters are optimized:

$$p^* = \arg \min_p \mathcal{L}_{\chi^2}(\hat{F}(p), F^{\text{obs}}) + \mathcal{L}_{\text{phys}}. \quad (12)$$

This formulation empirically yields stable inversion behavior under varying SNR conditions.

4 Experiments

4.1 Experimental Setup

This section details the experimental setup, including the dataset, model configuration, and physical module settings. All experiments are designed to evaluate the effect of structured physics embedding on generative performance and inverse stability.

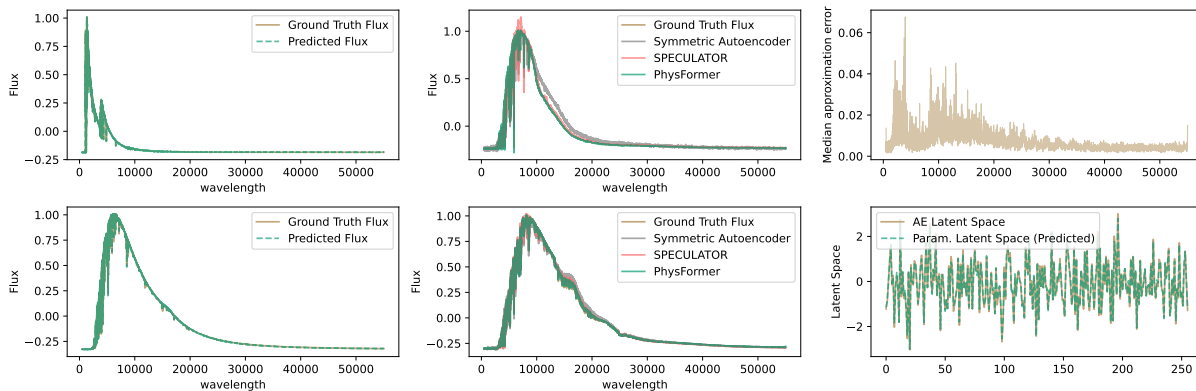


Figure 2: Visualization of Spectra Generated by PhysFormer. Left: comparison between PhysFormer-generated spectra and ground truth. Middle: comparison among PhysFormer, Symmetric Autoencoder, and SPECULATOR. Top right: median spectral error across wavelengths. Bottom right: visualization of the learned low-dimensional physical latent space.

Datasets. We use the PHOENIX stellar atmosphere model spectra, consisting of 26,747 spectra, each with length 9875, covering the ultraviolet, optical, and infrared bands. All spectra are normalized and partitioned into $N = 125$ non-overlapping wavelength patches, with each patch containing 79 consecutive wavelength points.

Model Configuration. In the physics-aware autoencoder, the encoder and decoder depths are set to 12 and 3, respectively, and the dimension of the physical latent space is 256.

Physical module. The stellar atmosphere is approximated as a semi-infinite plane-parallel layer. The optical depth is discretized into 64 layers, and angular integration is performed using Gauss–Legendre quadrature with 20 directions over the interval $[-1, 1]$.

Model	RMSE	MAE	R^2
PhysFormer (Ours)	0.0054	0.0033	0.9997
PhysGNN	0.1959	0.1622	0.7216
Symmetric Autoencoder	0.0200	0.0123	0.9956
SPECLATOR	0.0106	0.0064	0.9985
The Payne	0.0618	0.0357	0.9372
Kurucz-a1	0.0502	0.0204	0.9760

Table 1: Comparison of PhysFormer with Other Baselines

4.2 Spectral Modeling Performance of PhysFormer

As shown in Figure 2, the mean squared error between PhysFormer and the theoretical spectra is 4.40×10^{-5} . The error distributions in the ultraviolet (500–4000 Å) and infrared (7500–55,000 Å) bands are relatively stable and remain overall low. In contrast, the errors in the optical band (4000–7500 Å) are slightly higher, with the median error peaking within this interval. Overall, PhysFormer demonstrates accurate and stable spectral reconstruction for the majority of characteristic spectral lines.

4.3 Comparison with Existing Models

To comprehensively evaluate the effectiveness of PhysFormer, we selected several representative baseline methods that encompass different modeling approaches in high-dimensional scenarios.

The Payne [Ting *et al.*, 2019]. A representative data-driven framework for stellar spectrum generation and parameter inversion, which employs a MLP to directly learn the mapping from stellar parameters to spectral flux, without explicitly incorporating physical structures or intermediate physical quantities.

Kurucz-a1 [Li *et al.*, 2025]. We leverage its dual-encoder architecture to perform block-wise modeling of parameters and wavelength, and then concatenate the features to predict the spectral flux.

PhysGNN [Salehi and Giannacopoulos, 2022]. A physics-inspired graph neural network approach that represents physical variables as graph nodes and models their interactions via learned relational structures.

Symmetric Autoencoder [Gebran, 2024]. A symmetric autoencoder-based model that constructs a latent representation of stellar spectra and reconstructs the spectra through a mirrored decoder.

SPECULATOR [Alsing *et al.*, 2020]. A spectral emulation method that enables fast and accurate generation of galaxy spectra via PCA dimensionality reduction and neural network fitting.

We use three types of metrics to quantitatively assess the model performance: Root Mean Square Error (RMSE), Mean Absolute Error (MAE), and coefficient of determination (R^2). Table 1 and the middle panel of Figure 2 show that purely data-driven methods such as The Payne exhibit limited performance when generating ultra-high-dimensional, cross-band, high-resolution spectral fluxes from only four-dimensional stellar parameters. While SPECULATOR and symmetric autoencoders can capture the overall spectral shape, they exhibit poor stability and consistency in line-sensitive regions. In contrast, PhysFormer achieves lower prediction errors and more stable spectral responses under complex parameter variations.

Model Configuration	MSE(AE 200epoch)	MSE(P2F)	RTE Loss	ET Loss
PhysFormer (Ours)	6.24×10^{-5}	4.41×10^{-5}	5.16×10^{-5}	0.0195
w/o Physics Process	8.41×10^{-5}	4.28×10^{-5}	-	-
w/o Bottleneck	3.75×10^{-5}	0.0489	5.58×10^{-5} (AE) 3.09×10^{-5} (P2F)	0.0236(AE) 0.1210(P2F)
Smaller Bottleneck	8.60×10^{-4}	-	7.67×10^{-5}	0.0164
MLP Decoder	2.83×10^{-4}	-	1.17×10^{-4}	0.0189
Reduced Angular Integration	8.87×10^{-4}	-	2.66×10^{-5}	0.0160

Table 2: Ablation Experiment Results. AE refers to the autoencoder stage results (pretrained for 200 epochs), and P2F refers to the results from the parameter-to-flux prediction stage. RTE Loss represents the mean squared error of the radiative transfer equation residuals, while ET Loss denotes the mean squared error of the energy theorem residuals. Due to the limited training epochs in the AE stage, its errors are generally higher than those in the P2F stage.

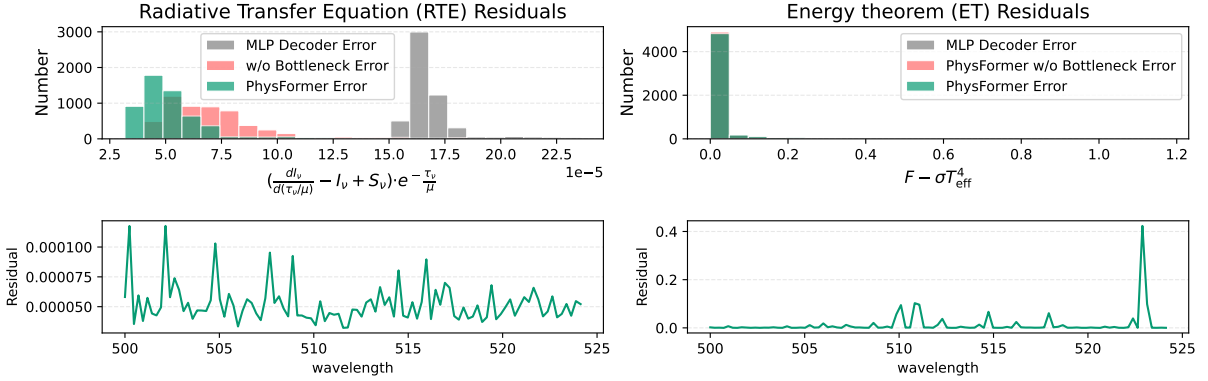


Figure 3: Residual Distributions of RTE and ET on the Test Set. Top row: Residual distributions of the Radiative Transfer Equation (RTE) and Energy Theorem (ET) for the three models: PhysFormer, PhysFormer without Bottleneck, and MLP Decoder. Bottom row: Absolute residual distributions of RTE and ET for the first 100 wavelength points for PhysFormer.

4.4 Ablation Study

To assess the contribution of each component in PhysFormer, we perform ablation studies on the physical modules, latent structure, and numerical integration (Table 2).

PhysFormer w/o Physics Process. In this variant, the physical generation module and its associated physical constraints are removed, and latent variables are directly decoded into spectra. Although this model still attains a mean squared error on the order of 1×10^{-5} during both the autoencoder training stage and the parameter-to-spectrum prediction stage, it essentially degenerates into a purely data-driven model, with the learned representations primarily capturing empirical correlations rather than possessing explicit physical interpretability. This variant exhibits substantially larger parameter estimation errors in the inversion task compared to the full PhysFormer, as discussed in Section 4.5.

PhysFormer w/o Bottleneck. To verify the necessity of the low-dimensional latent space, we removed the Bottleneck module, directly connecting the encoder output to the decoder. Although the autoencoder reconstruction error is very low (3.75×10^{-5}), the mean squared error increases sharply to 0.0489 during the parameter-to-spectrum prediction stage. This indicates that the four-dimensional stellar fundamental parameters are difficult to directly map to the ultra-high-dimensional stellar spectra, and the Bottleneck de-

sign plays a crucial role in balancing reconstruction capability with the physical interpretability of the latent space.

Smaller Bottleneck. We reduced the dimensionality of the low-dimensional latent space from 256 to 128. Experimental results indicate that excessive compression of the latent space constrains the model’s expressive capacity, causing the spectral reconstruction error of the autoencoder to increase by more than an order of magnitude. This indicates that selecting an appropriate latent space dimensionality is crucial for preserving physically meaningful variations and alleviating the difficulty of parameter-to-spectrum mapping.

MLP Decoder. The Transformer-style decoder was replaced with an MLP decoder. Although the model can capture the overall spectral structure, both prediction accuracy and generalization were inferior to the Transformer decoder, indicating the advantage of Transformer architectures in modeling long-range dependencies in high-dimensional spectral sequences.

Reduced Angular Integration. The number of Gaussian directions considered in the semi-infinite plane-parallel atmosphere was reduced from 20 to 4. The results show a significant decrease in spectral accuracy, highlighting the importance of sufficiently accurate numerical integration for maintaining spectral generation performance.

In addition, the RTE Loss and ET Loss not explicitly la-

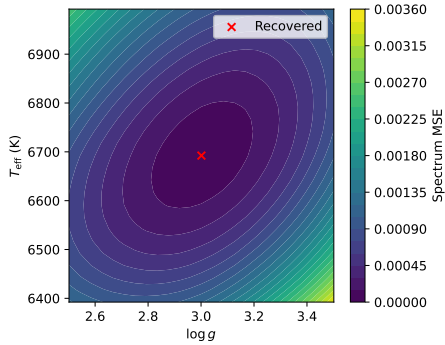


Figure 4: Loss landscape in $T_{\text{eff}}\text{-}\log g$ space for a single observed spectrum. Color indicates the spectrum reconstruction MSE. The red cross marks the recovered parameter. The elongated and tilted contours indicate a strong degeneracy between the two parameters.

beled in Table 2 correspond to the autoencoder phase. All models containing physical modules could compute the physical equation losses and maintain them at low levels, indicating that the model design remains numerically consistent with the embedded physical constraints. Additional checks confirm that the true absorption and scattering coefficients remain non-negative, and the generated temperature distributions remain within the bounds of the PHOENIX theoretical spectra, suggesting that PhysFormer learns physically consistent representations of intermediate quantities. It should be noted that flux prediction accuracy remains the primary evaluation criterion. Models with a lower RTE Loss may still produce inaccurate emergent fluxes, which highlights the necessity of incorporating global physical constraints and physically structured latent representations.

Figure 3 illustrates that PhysFormer (Ours) achieves the lowest and most tightly distributed RTE residuals, whereas the MLP Decoder exhibits substantially larger residuals. Regarding the energy theorem, all three models show comparable performance, indicating that the ET loss is primarily governed by the physical module.

4.5 Parameter Inversion Experiments

In the parameter inversion experiments, we compared the performance of PhysFormer with PhysFormer w/o Physics Process under different SNR conditions. Unlike inversion studies that rely on strong priors or empirical templates, we consider a particularly challenging inversion setting characterized by: (1) low-SNR observations, where the inversion process must recover stellar parameters under significant noise interference; (2) The model relies solely on the spectra for parameter estimation, which significantly increases the risk of parameter degeneracy, i.e., the existence of distinct parameter combinations that produce nearly indistinguishable spectra (Figure 4). This problem constitutes a highly nonlinear, strongly degenerate, and noise-sensitive inverse problem.

Figure 5 illustrates stellar parameter recovery by the two models. The top panel presents a rare star with solar metallicity and enhanced α -elements ($T_{\text{eff}} = 4300$ K, $\log g = 5.5$, $[\text{Fe}/\text{H}] = 0.0$, $[\alpha/\text{Fe}] = 1.2$). For certain rare stars, PhysFormer maintains high inversion accuracy, producing

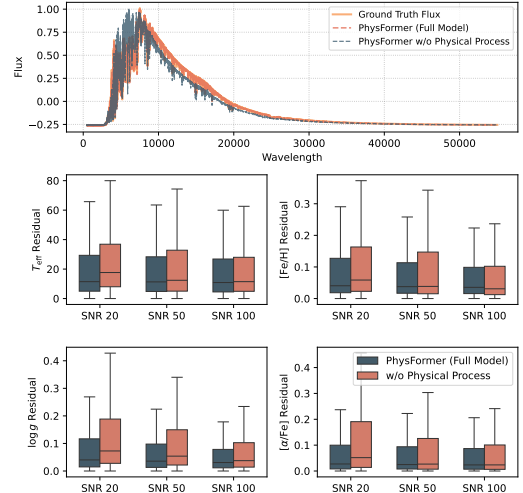


Figure 5: Example of Parameter Inversion Results and Error Distributions. Top: Example spectra generated from the inverted parameters, comparing the output of PhysFormer with PhysFormer w/o Physics Process. Bottom: Distributions of absolute errors in the inversion of four-dimensional stellar parameters under different signal-to-noise ratio (SNR) conditions for the two models.

spectra from the inferred parameters that more closely match the theoretical spectra. As shown in the bottom panel, the overall residual distribution of parameters inferred by PhysFormer is narrower and lower, and remains stable across different SNR conditions, indicating that the physically structured constraints contribute to improved robustness of the inversion process. Although all parameters remain challenging due to unavoidable degeneracies, PhysFormer significantly mitigates unstable inversion compared to baselines.

5 Conclusion

This work proposes PhysFormer, a physics-consistent, generative-modeling framework for stable spectral modeling and accurate parameter inversion, even when the underlying high-dimensional physical fields are unknown. Unlike conventional PINNs that primarily rely on external physics-based losses, PhysFormer directly embeds the physical generation process into the network and uses a low-dimensional, physically interpretable latent space to learn key radiative transfer quantities, producing predictions that are consistent at both data and physics levels. We validate its performance on an ultra-long stellar spectral dataset spanning ultraviolet, visible, and infrared bands with 9,875 wavelength points. Experiments show that PhysFormer achieves superior stability and consistency, even in spectrally sensitive regions. More broadly, by replacing the equations or constraints in the physics module while keeping the overall architecture and latent space unchanged, PhysFormer can be extended, in principle, to other high-dimensional systems with unobservable physical quantities. This work thus illustrates a general framework for embedding physical processes directly into generative modeling, providing a practical approach for physics-consistent modeling of complex scientific systems.

References

- [Alsing *et al.*, 2020] Justin Alsing, Hiranya Peiris, Joel Leja, ChangHoon Hahn, Rita Tojeiro, Daniel Mortlock, Boris Leistedt, Benjamin D Johnson, and Charlie Conroy. Speculator: Emulating stellar population synthesis for fast and accurate galaxy spectra and photometry. *The Astrophysical Journal Supplement Series*, 249(1):5, 2020.
- [Cheridito *et al.*, 2025] Patrick Cheridito, Jean-Loup Dupret, and Donatien Hainaut. Deep learning for continuous-time stochastic control with jumps. In *The Thirty-ninth Annual Conference on Neural Information Processing Systems*, 2025.
- [Corral *et al.*, 2023] LJ Corral, CR Fierro-Santillán, SG Navarro, et al. Stellar parameter estimation in o-type stars using artificial neural networks. *Astronomy and Computing*, 45:100760, 2023.
- [Dahlbüdding *et al.*, 2024] David Dahlbüdding, Karan Molaverdikhani, Barbara Ercolano, and Tommaso Grassi. Approximating rayleigh scattering in exoplanetary atmospheres using physics-informed neural networks. *Monthly Notices of the Royal Astronomical Society*, 533(3):3475–3483, 2024.
- [De Ryck and Mishra, 2022] Tim De Ryck and Siddhartha Mishra. Error analysis for physics-informed neural networks (pinns) approximating kolmogorov pdes. *Advances in Computational Mathematics*, 48(6):79, 2022.
- [Dosovitskiy *et al.*, 2021] Alexey Dosovitskiy, Lucas Beyer, Alexander Kolesnikov, Dirk Weissenborn, Xiaohua Zhai, Thomas Unterthiner, Mostafa Dehghani, Matthias Minderer, Georg Heigold, Sylvain Gelly, Jakob Uszkoreit, and Neil Houlsby. An image is worth 16x16 words: Transformers for image recognition at scale. In *International Conference on Learning Representations*, 2021.
- [Gebran, 2024] Marwan Gebran. Generating stellar spectra using neural networks. *Astronomy*, 3(1):1–13, 2024.
- [Higgins *et al.*, 2017] Irina Higgins, Loic Matthey, Arka Pal, Christopher Burgess, Xavier Glorot, Matthew Botvinick, Shakir Mohamed, and Alexander Lerchner. beta-vae: Learning basic visual concepts with a constrained variational framework. In *International conference on learning representations*, 2017.
- [Hubeny and Mihalas, 2014] Ivan Hubeny and Dimitri Mihalas. *Theory of stellar atmospheres: An introduction to astrophysical non-equilibrium quantitative spectroscopic analysis*. Princeton University Press, 2014.
- [Jaegle *et al.*, 2021] Andrew Jaegle, Felix Gimeno, Andy Brock, Oriol Vinyals, Andrew Zisserman, and Joao Carreira. Perceiver: General perception with iterative attention. In *International conference on machine learning*, pages 4651–4664. PMLR, 2021.
- [Jagtap and Karniadakis, 2020] Ameya D. Jagtap and George Em Karniadakis. Extended physics-informed neural networks (xpinn): A generalized space-time domain decomposition based deep learning framework for nonlinear partial differential equations. *Communications in Computational Physics*, 28(5):2002–2041, 2020.
- [Jagtap *et al.*, 2020] Ameya D. Jagtap, Ehsan Kharazmi, and George Em Karniadakis. Conservative physics-informed neural networks on discrete domains for conservation laws: Applications to forward and inverse problems. *Computer Methods in Applied Mechanics and Engineering*, 2020.
- [Li *et al.*, 2021] Zongyi Li, Nikola Borislavov Kovachki, Kamyar Azizzadenesheli, Burigede Iiu, Kaushik Bhat-tacharya, Andrew Stuart, and Anima Anandkumar. Fourier neural operator for parametric partial differential equations. In *International Conference on Learning Representations*, 2021.
- [Li *et al.*, 2022] Zhuohan Li, Gang Zhao, Yuqin Chen, Xilong Liang, and Jingkun Zhao. The stellar parameters and elemental abundances from low-resolution spectra–i. 1.2 million giants from lamost dr8. *Monthly Notices of the Royal Astronomical Society*, 517(4):4875–4891, 2022.
- [Li *et al.*, 2025] Jiadong Li, Mingjie Jian, Yuan-Sen Ting, and Gregory M Green. Differentiable stellar atmospheres with physics-informed neural networks. In *ICML 2025 Workshop on Machine Learning for Astrophysics*, 2025.
- [Liu *et al.*, 2025] Ziti Liu, Yang Liu, Xunshi Yan, Wen Liu, Han Nie, Shuaiqi Guo, and Chen-an Zhang. Automatic network structure discovery of physics informed neural networks via knowledge distillation. *Nature Communications*, 16(1):9558, 2025.
- [Long *et al.*, 2019] Zichao Long, Yiping Lu, and Bin Dong. Pde-net 2.0: Learning pdes from data with a numeric-symbolic hybrid deep network. *Journal of Computational Physics*, 399:108925, 2019.
- [Mao *et al.*, 2020] Zhiping Mao, Ameya D. Jagtap, and George Em Karniadakis. Physics-informed neural networks for high-speed flows. *Computer Methods in Applied Mechanics and Engineering*, 2020.
- [Meng *et al.*, 2020] Xuhui Meng, Zhen Li, Dongkun Zhang, and George Em Karniadakis. Ppinn: Parareal physics-informed neural network for time-dependent pdes. *Computer Methods in Applied Mechanics and Engineering*, 370:113250, 2020.
- [Mi and Sun, 2024] Yuan Mi and Hao Sun. Spatiotemporal learning on cell-embedded graphs. *arXiv preprint arXiv:2409.18013*, 2024.
- [Mishra and Molinaro, 2021] Siddhartha Mishra and Roberto Molinaro. Physics informed neural networks for simulating radiative transfer. *Journal of Quantitative Spectroscopy and Radiative Transfer*, 270:107705, 2021.
- [Nasir *et al.*, 2025] Karthika Nasir, Rahul Menon, and Sneha Iyer. A mathematical and algorithmic review of physics-informed neural networks for scientific computing. 2025.
- [Press and Teukolsky, 2007] William H Press and Saul A Teukolsky. *Numerical recipes with source code CD-ROM 3rd edition: the art of scientific computing*. Cambridge University Press, 2007.
- [Raissi *et al.*, 2019] Maziar Raissi, Paris Perdikaris, and George E Karniadakis. Physics-informed neural networks:

- A deep learning framework for solving forward and inverse problems involving nonlinear partial differential equations. *Journal of Computational physics*, 378:686–707, 2019.
- [Raissi *et al.*, 2020] Maziar Raissi, Alireza Yazdani, and George Em Karniadakis. Hidden fluid mechanics: Learning velocity and pressure fields from flow visualizations. *Science*, 367(6481):1026–1030, 2020.
- [Rao *et al.*, 2023] Chengping Rao, Pu Ren, Qi Wang, Oral Buyukozturk, Hao Sun, and Yang Liu. Encoding physics to learn reaction–diffusion processes. *Nature Machine Intelligence*, 5(7):765–779, 2023.
- [Salehi and Giannacopoulos, 2022] Yasmin Salehi and Dennis Giannacopoulos. Physgnn: A physics–driven graph neural network based model for predicting soft tissue deformation in image–guided neurosurgery. *Advances in Neural Information Processing Systems*, 35:37282–37296, 2022.
- [Sedaghat *et al.*, 2021] Nima Sedaghat, Martino Romaniello, Jonathan E Carrick, and François-Xavier Pineau. Machines learn to infer stellar parameters just by looking at a large number of spectra. *Monthly Notices of the Royal Astronomical Society*, 501(4):6026–6041, 01 2021.
- [Ting *et al.*, 2019] Yuan-Sen Ting, Charlie Conroy, Hans-Walter Rix, and Phillip Cargile. The payne: self-consistent ab initio fitting of stellar spectra. *The Astrophysical Journal*, 879(2):69, 2019.
- [Wan *et al.*, 2025] Han Wan, Rui Zhang, Qi Wang, Yang Liu, and Hao Sun. Pesanet: Physics-encoded spectral attention network for simulating pde-governed complex systems. In James Kwok, editor, *Proceedings of the Thirty-Fourth International Joint Conference on Artificial Intelligence, IJCAI-25*, pages 7751–7759. International Joint Conferences on Artificial Intelligence Organization, 8 2025. Main Track.
- [Yang *et al.*, 2021] Liu Yang, Xuhui Meng, and George Em Karniadakis. B-pinns: Bayesian physics-informed neural networks for forward and inverse pde problems with noisy data. *Journal of Computational Physics*, 425:109913, 2021.
- [Zeng *et al.*, 2025] Bocheng Zeng, Qi Wang, Mengtao Yan, Yang Liu, Ruizhi Chengze, Yi Zhang, Hongsheng Liu, Zidong Wang, and Hao Sun. PhyMPGN: Physics-encoded message passing graph network for spatiotemporal PDE systems. In *The Thirteenth International Conference on Learning Representations*, 2025.
- [Zhu *et al.*, 2022] Wei Zhu, Wesley Khademi, Efstathios G Charalampidis, and Panayotis G Kevrekidis. Neural networks enforcing physical symmetries in nonlinear dynamical lattices: The case example of the ablowitz–ladik model. *Physica D: Nonlinear Phenomena*, 434:133264, 2022.